Journal of Membrane Science 495 (2015) 216–225

Contents lists available at ScienceDirect

Journal of Membrane Science

journal homepage: www.elsevier.com/locate/memsci

Solvent permeation behavior of PDMS grafted γ-alumina membranes

Cheryl R. Tanardi [a,b], Ivo F.J. Vankelecom [b], Ana F.M. Pinheiro [a], Kishore K.R. Tetala [a], Arian Nijmeijer [a], Louis Winnubst [a,*,1]

[a] Inorganic Membranes, MESA+ Institute for Nanotechnology, University of Twente, P.O. Box 217, 7500 AE Enschede, The Netherlands
[b] Centre for Surface Chemistry and Catalysis, Department of Molecular and Microbial Systems, KU Leuven, Kasteelpark Arenberg 23, PO Box 2461, 3001 Leuven, Belgium

ARTICLE INFO

Article history:
Received 5 May 2015
Received in revised form
27 July 2015
Accepted 1 August 2015
Available online 14 August 2015

Keywords:
Solvent resistant nanofiltration
PDMS
Alumina
Membrane
Grafting
Transport

ABSTRACT

Solvent permeability in polymer grafted ceramic membranes was described by incorporating solvent sorption terms into the Hagen–Poiseuille equation. Two types of ceramic membranes grafted with a relative short or long PDMS chain ($n=10$ and $n=39$), which differed in pore size, were examined. Sorption was measured "ex situ" using a pure PDMS phase. The results show that curves of flux versus transmembrane pressure were identical for all solvents studied if flux values are corrected for viscosity as well as sorption of the solvent. It is suggested that the permeable volume of the membrane reduces by swelling of the grafted organic moiety by the solvent used. This model provides a way to predict the performance of grafted porous membranes for solvent filtration.

1. Introduction

Solvent resistant nanofiltration (SRNF) or organic solvent nanofiltration (OSN) is a potential separation technology for e.g. the recycling of solvents and the recovery of products from reaction solvents [1]. For SRNF, a chemically stable membrane is required to endure the rather aggressive operation environment. Modification of mesoporous ceramic membranes by means of grafting is an interesting way to prepare a chemically stable nanofiltration membrane. In the grafting process, the macromolecules are linked to the membrane surface by a covalent bond, resulting in a chemically stable modified ceramic membrane. The surface wettability of the membrane can be tuned by grafting a suitable polymer with the desired hydrophobicity. In the same time, pore size tuning can be realized by grafting macromolecules inside the ceramic pores.

In literature several examples are given on modification of porous inorganic membranes by grafting for various applications. Leger et al. [2] used silicone oil (viscosity 545 mPa) to graft the surface of alumina membranes with a pore size of 5 nm for gas permeation and pervaporation. Faibish and Cohen [3] grafted polyvinylpyrrolidone on zirconia membranes for oil-in-water emulsion treatment. Free-radical graft polymerization was performed by using a vinyl silane as linker to the zirconia membranes. A reduction in pore size of around 25% after grafting was claimed. Yoshida and Cohen [4] grafted y-alumina membranes (pore size 5 nm) by using vinyl acetate or vinyl pyrrolidone monomers. Yoshida and Cohen [5] grafted vinyl acetate or vinyl pyrrolidone to silica membranes (pore size of 20 nm) by free radical graft polymerization for pervaporation of methyl-tertiary-butyl ether from water. Popat et al. [6] grafted polyethylene glycol to straight pore alumina membranes ("anodisc") using a silane coupling agent. Sang Won et al. [7] grafted polyethylene glycol to render straight pore alumina membranes for anti-fouling properties. The pore sizes of the bare alumina, used in [6] and [7], are in the order of 25–80 nm, while the grafted membranes are still in the ultrafiltration range.

Pinheiro et al. [8] developed nanofiltration membranes by grafting PDMS in the pores of γ-alumina membranes (pore size 5 nm) using aminopropylethoxysilane as the linker and (mono (2,3-epoxy) polyetherterminated polydimethylsiloxane with an average number of repeating monomers (n) of 10 and a viscosity of 10–50 mPa. Tanardi et al. [9] grafted PDMS with an average number of repeating monomers (n) of 39 on the same type of mesoporous (pore size 5 nm) γ-alumina layer, supported on macro porous α-alumina, with 3-mercaptopropyltriethoxysilane as linker.

Detailed knowledge of major parameters influencing the solvent transport of grafted ceramic membranes is very important in

* Corresponding author. Fax: +31 534892336.
E-mail address: a.j.a.winnubst@utwente.nl (L. Winnubst).
[1] www.utwente/tnw/im

http://dx.doi.org/10.1016/j.memsci.2015.08.004
0376-7388/

order to predict their permeation behavior for various solvents. Castro et al. [10] studied the effect of different types of solvents on the permeability of an ultrafiltration membrane, prepared by grafting of PVP inside the pores of a macroporous silica support with a native pore diameter of 410 nm. It was found that the permeability of nonpolar solvents, like cyclohexane and toluene, was higher than the permeability of polar solvents, like propanol, water, and ethanol, for the hydrophilic PVP grafted membranes, as opposite to what was expected.

An interesting behavior of modified ceramic membranes prepared via grafting of macromolecules inside the pores is their response towards the applied pressure. Castro et al. [11] observed a shear-rate flow induced behavior of the PVP grafted macroporous ceramic substrate with d_{avg} of 410 nm due to the mobility of the grafted polymeric chain. The effect of shear rate on the permeability of the grafted membrane was described as a condition in which the membrane is experiencing a more open membrane structure due to the movement of the grafted moieties in the direction of the feed flow, resulting in an exponential increase in the membrane permeability towards the trans-membrane pressure.

In this study, the effect of viscosity as well as sorption of the solvent on the transport behavior were investigated for two types of PDMS-grafted membranes with respectively a relative short and long chain length ($n=10$ and $n=39$). PDMS was selected as it has been proven to be an excellent material for SRNF applications [8,9,12–14]. The permeability was studied by means of permeation tests at operating pressures between 1 and 20 bar to investigate the effect of trans-membrane pressure on the membrane permeability. Various solvents were used to study the effect of different solvent types on the membrane permeation behavior. Permeation tests at elevated temperature were conducted to study the effect of temperature on the membrane permeability. A model is proposed to describe the permeation of pure solvents through these membranes.

2. Existing transport models for porous and dense membranes

Two models are generally used to describe solvent transport through membranes [15]. The first one is the pore-flow model, in which the membrane is regarded to have defined open pores from the feed side to the permeate side. Darcy's Law, often referred to as the pore-flow or viscous-flow model, describes liquid permeation through porous media as a function of the trans-membrane pressure (TMP)

$$J = \frac{k}{\mu}\frac{\Delta P}{l} \tag{1}$$

where J is the solvent flux, k the permeability constant, μ the fluid viscosity, ΔP the trans-membrane pressure, and l the membrane thickness.

For viscous flow, the Darcy's law can be combined with the Hagen–Poiseuille equation

$$J = k\frac{\Delta P}{\mu} \tag{2}$$

with

$$k = \frac{\varepsilon {r_p}^2}{8\tau l} \tag{3}$$

where J is the solvent flux, ΔP the trans-membrane pressure, μ the solvent viscosity, and k the membrane permeability constant representing the structural properties of the membrane with ε the membrane porosity, r_p the membrane average pore diameter, τ the membrane tortuosity, and l the membrane thickness.

If there are no pores identified in the membrane, the solution–diffusion model is generally used [15]. This means that the transport of liquids occurs via free volume elements between polymeric chains which can appear and disappear as a function of time and place according to the movement of the solvent [16]. The model assumes that pressure is constant through the membrane and the driving force of solvent transport is the chemical activity difference between the feed and permeate side of the dense membrane. The solution–diffusion equation is as follows:

$$J_i = \frac{D_i K_i}{l}\left[a_{if} - a_{ip}\exp\left(\frac{-v_i\left(P_f - P_p\right)}{R_g T}\right)\right] \tag{4}$$

where J_i represents the solvent flux, l the membrane thickness, D_i the diffusion coefficient of solvent or solute i through the membrane, K_i the partition coefficient, a_{if} and a_{ip} are the activities of species i in respectively feed and permeate, v_i the partial molar volume of specimen i, P_f and P_p the pressures at feed and permeate side, R_g the gas constant and T the temperature. If a pure solvent is used, then the a_{if} is 1 and v_i is 1, while the a_{ip} is 0. Thus, the equation becomes

$$J_i = \frac{D_i K_i}{l}\left[1 - \exp\left(\frac{-(\Delta P - \Delta\pi)}{R_g T}\right)\right] \tag{5}$$

where $\Delta\pi$ stands for the osmotic pressure [17].

When the difference between the applied and osmotic pressure is small, the equation can be written as

$$J_i = \frac{D_i K_i}{R_g l T}(\Delta P - \Delta\pi) = S_i(\Delta P - \Delta\pi) \tag{6}$$

where S_i is a solvent permeability constant of solvent or solute i.

The pore-flow and the solution–diffusion models are commonly used for aqueous applications [15,18,19]. For SRNF membranes, both pore-flow and solution–diffusion models have been used in literature to describe the transport behavior for PDMS membranes. Vankelecom et al. [16] found that a viscous flow model can be used to describe the permeation of pure solvents through PDMS membranes by taking into account membrane swelling. This finding was later confirmed by Robinson et al. [20], who successfully used a pore-flow model to describe the transport behavior of PDMS membranes for nonpolar solvents based on the reasoning that the swollen PDMS layer may form a pore-like structure in the presence of nonpolar solvents. Meanwhile, Zeidler et al. [21] found that a viscous flow behavior was observed for PDMS membranes in the presence of swelling solvents like n-heptane and THF. On the other hand, in the presence of non-swelling solvents, like ethanol, it was proposed that the rejection of PDMS might be closer to that of the solution–diffusion mechanism. Postel et al. [22] used the solution–diffusion model to describe the negative rejections of dye solutes in ethanol through dense PDMS membranes. No prior study is found in the literature to investigate the use of these models for modeling of the transport behavior of grafted ceramic membranes.

3. Experimental procedures

Three types of membranes were investigated. All membranes were in the form of flat discs with a diameter of 20 mm and a total thickness of 2.5 mm. The first series of membranes (M1) consisted of a mesoporous γ-Al_2O_3 layer with a pore diameter of 5 nm and 3 μm thickness, supported on macroporous α-Al_2O_3 supports [23,24]. The second series (M2) consisted of macroporous α-Al_2O_3 supports, coated with a 3 μm thick mesoporous (5 nm) γ-Al_2O_3 layer, which is modified with 3-aminopropyltriethoxysilane

followed by mono(2,3-epoxy)polyetherterminated polydimethylsiloxane ($n=10$). Details of the membrane fabrication procedures for M2 were described in [8]. The third series of membranes (M3) consisted of macroporous α- Al_2O_3 supports, coated with a 3 μm thick mesoporous (5 nm) γ-Al_2O_3 layer and further modified with 3-mercaptopropyl triethoxysilane followed by monovynil terminated polydimethylsiloxane ($n=39$). Details of the membrane fabrication procedures for M3 were described in [9]. SEM-EDX analysis by a Thermo-Noran instrument was used to identify the morphology of the grafted membranes.

Permeability tests were performed using a high pressure dead-end stainless steel permeation set-up at operating pressures between 1 and 20 bar [25]. The cell was filled with solvent and nitrogen was used to pressurize the cell. Permeate fluxes (J in L m^{-2} h^{-1}) were obtained by measuring the weight of the collected permeate as a function of time.

Pure solvent flux tests were conducted with different solvents. Octane (98% purity), cyclooctane (> 99%), p-xylene (> 99%), and n-hexane (> 99%) were purchased from Sigma-Aldrich. Toluene (100%), ethyl acetate (99.9%), and isopropanol (100%) were purchased from VWR. Zeolite A (molecular mesh 4–8 nm) was purchased from Sigma-Aldrich to dry all chemicals. Table 1 gives some physical characteristics of these solvents.

After each permeation test, the samples were rinsed thoroughly with ethanol 3 times and soaked in fresh ethanol for 24 h before being dried in a vacuum oven for 1 h at 110 °C. Membranes were cooled down for 24 h in a vacuum oven at 30 °C prior to soaking for 8 h in the solvent to be tested before the permeation test was started. All measurements were performed on three samples for each type of membrane and two times for each sample. The influence of temperature was studied by performing permeability tests up to 70 °C at 6 bars for octane, toluene, and isopropanol.

Contact angle measurements, hexane flux tests at 10 bar, and molecular weight cut off (MWCO) measurements were used to control the membrane condition before and after the permeation tests with series of solvents.

Contact angles were measured by the static sessile drop method by the Data Physics Optical Contact Angle (OCA 20) instrument. 5 μL of water was dropped respectively at a speed of 2 μ l s^{-1} on the membranes surface using a *Hamilton Microliter* syringe. Measurements were taken on 5 different spots on the membrane surface.

MWCO measurements were performed with the same dead-end permeation set-up as used for the permeation tests by using polyethylene glycol (PEG, Fluka) with molecular weights of 200, 400, 600, and 1000 g/mol respectively as probe solutes in toluene. The rejection test was performed until an equilibrium retention value was reached. All measurements were performed on three different membrane samples for each type of membrane. The feed solution was stirred at 500 rpm to avoid any concentration polarization. The feed concentration was set at 8000 ppm. Solute concentrations in the permeate and feed solution were analyzed by a Thermo Electron Corporation HPLC with a C8 econosphere column connected to an Evaporative Light Scattering Detector 2000 ES [26]. A nebulizer temperature of 95 °C, a gas flow of 2.5 L/min, a column temperature of 40 °C and a sample volume of 20 μL were used. Methanol–water (4:1) was used as the eluent for the HPLC. The feed and permeate solute concentration (C_f and C_p) were determined for different MWs as a function of the total peak area from the electrical potential difference plot against the retention time. The rejection percentage (R) was calculated from the following equation: $R=(1-C_p/C_f)\times 100\%$, where C_p and C_f are the solute concentrations in the permeate and feed solution, respectively. The MWCO value is determined as a solute molecular weight for which a 90% retention is observed.

It was not possible to directly measure the solvent sorption behavior of PDMS in different solvents using the as-prepared membranes. Thus, to indicate the sorption tendency of PDMS in different solvents, sorption tests were performed on non-grafted PDMS samples and the values were normalized towards the PDMS sorption of one reference solvent. This provides an indication of the affinity between PDMS and different types of solvent. For this sorption study PDMS samples were prepared by dissolving 10 wt% of RTV-615 A in hexane. PDMS RTV-615 A and RTV-615B were purchased from Momentive Performance Materials Belgium. 1% of RTV-615B was added into the solution and pre-polymerized at 60 °C for 1 h. The pre-polymerized solution was then poured into a flat petri dish and the solvent was allowed to evaporate overnight. The samples were put into a vacuum oven at 110 °C for 8 h to complete the polymerization. Afterwards, the samples were cooled down and cut into 0.2 mm thick discs with a diameter of 20 mm each. Sorption tests were performed by immersing the PDMS samples into 10 ml of solvents at different temperatures. The mass of the PDMS sample was weighed before and after the immersion, by wiping the solvent quickly from the external surface after immersion. The sorption value (S) in cm^3/g was defined as: $S=((m_e-m_o)/m_o)/\rho_s$, with m_o is the dry mass of PDMS (g), m_e the mass of swollen PDMS (g), and ρ_s the density of the solvents (g/cm^3). Measurements were performed three times for each type of solvent.

4. Results and discussion

4.1. Membrane structure and stability

In previous work it was shown that a chemical bond exists between γ-alumina and the grafted organic moieties [8,9]. The thickness of the polymer grafted layer was analyzed by SEM-EDX which results are given in Fig. 1. The SEM pictures of the M2 and M3 membranes in Fig. 1(a) and (d) show the modified γ-Al_2O_3 substrate supported on top of α-Al_2O_3. Al and Si EDX mapping of the M2 and M3 membranes are given in Fig. 1. As can be seen from

Table 1
Physical properties of the solvents used for permeability tests [29–34]

Name	Molecular shape	Viscosity (mPa s at 20 °C)	Dipole moment (D)	Dielectric constant (ε)	Surface tension (mN/m at 20 °C)	Molar volume (cm^3/mol)	Vapor pressure (mmHg at 20 °C)
Hexane	Linear	0.31	0.08	1.89	18	130.58	129.1
Octane	Linear	0.54	0	1.95	22	162.49	13.9
Cyclooctane	Cyclic	2.13	0	2.12	32	107.91	4.4
p-Xylene	Aromatic	0.64	0.07	2.27	29	123.31	7.6
Toluene	Aromatic	0.59	0.34	2.38	30	105.91	26.3
Ethyl acetate	Branched linear	0.45	1.88	6.02	24	97.68	109.1
Isopropanol	Branched linear	2.39	1.66	19.92	21	76.90	78.2

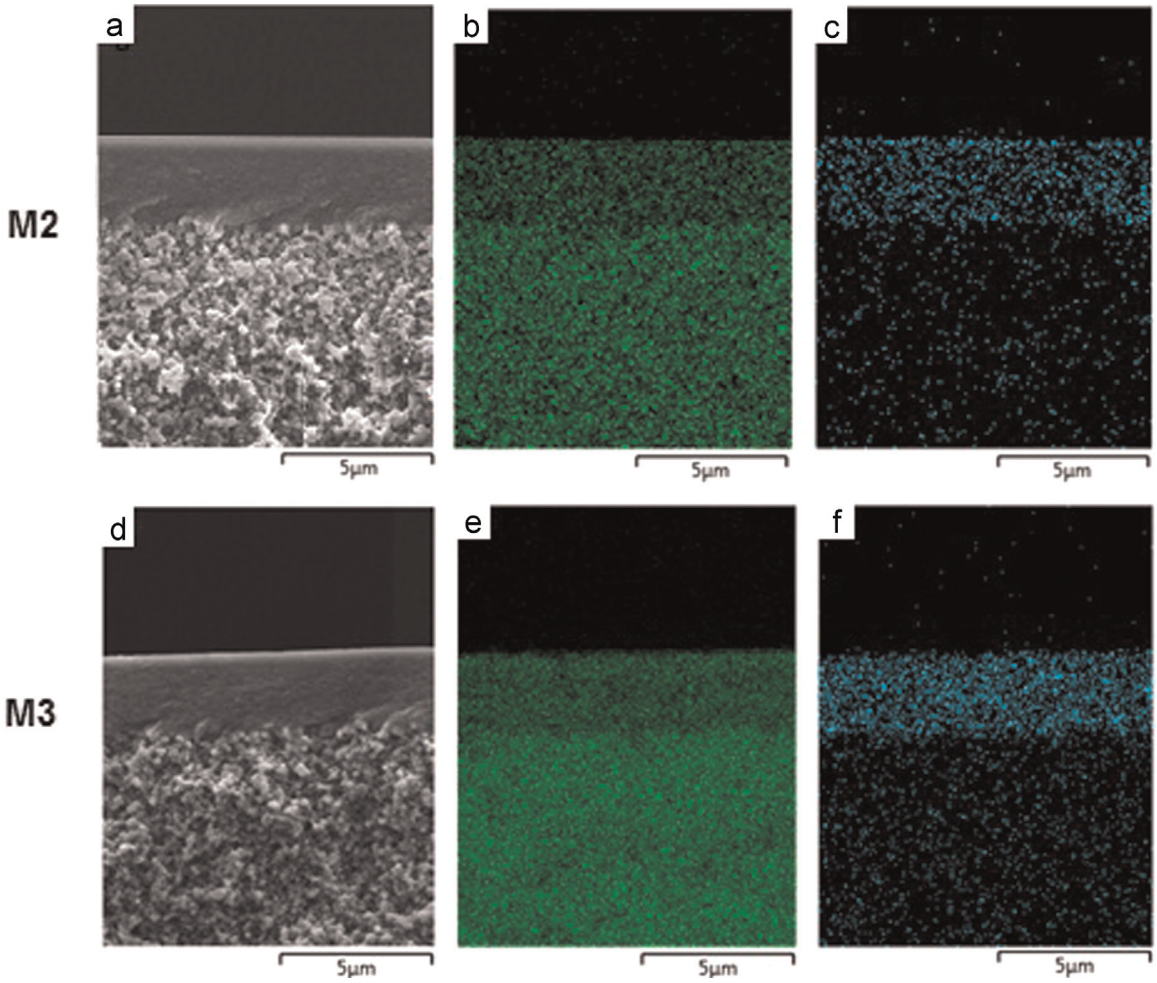

Fig. 1. SEM and EDX results for M2 membrane (a) SEM picture, (b) Al mapping (green), (c) Si mapping (blue) as well as for M3 membrane (d) SEM picture, (e) Al mapping (green), (f) Si mapping (blue). (For interpretation of the references to color in this figure legend, the reader is referred to the web version of this article.)

Table 2
Membrane characteristics.

Code	Material	Water contact angle (°)[a]	Water contact angle (°)[b]	MWCO (Da)[a]	MWCO (Da)[b]	Hexane flux at 10 bar ($L\,m^{-2}\,h^{-1}$)[a]	Hexane flux at 10 bar ($L\,m^{-2}\,h^{-1}$)[b]
M1	y-alumina	~0	~0	7500[35]	N/A	87.1 ± 2.7	87.0 ± 2.5
M2	y-alumina/ PDMS $n=10$	94 ± 1	94 ± 1	600	600	48.0 ± 1.9	47.9 ± 1.8
M3	y-alumina/ PDMS $n=39$	95 ± 1	95 ± 1	400	400	26.7 ± 1.0	26.6 ± 0.9

[a] Values, measured prior to permeability experiments on the solvents as indicated in Table 1
[b] Values, measured after all permeability experiments were performed

the EDX picture, the grafting occurs throughout the y-alumina layer with an observed thickness of about 3 μm for the selective layer for both M2 and M3 membranes.

In order to conduct proper solvent transport studies, it is important that the membranes remain stable and retain their (micro) structure during all tests. Therefore, some membrane characteristics were analyzed before and after these permeation tests: water contact angle, hexane flux and MWCO of PEG in toluene. These results are summarized in Table 2.

As can be seen from this table, water contact angle, MWCO and hexane permeability are similar before and after all permeation tests without any significant differences. All these results showed that all membranes remained stable during the whole testing period.

Both M2 and M3 showed lower MWCO values as compared to the unmodified γ-alumina membranes due to the presence of the grafted PDMS in the pores. M3 showed a lower MWCO than M2. On the other hand, the pure hexane permeability through the M2 membranes is higher than that of M3. This is an indication that M2 membranes have a more open structure than M3 membranes. This will be discussed further in the next section.

4.2. Permeability performance

Pure solvent flux data at room temperature for M2 and M3 membranes at different trans-membrane pressures (TMP) are given in Fig. 2. The flux values, as presented in Fig. 2, are the average equilibrium values of measurements performed on three different

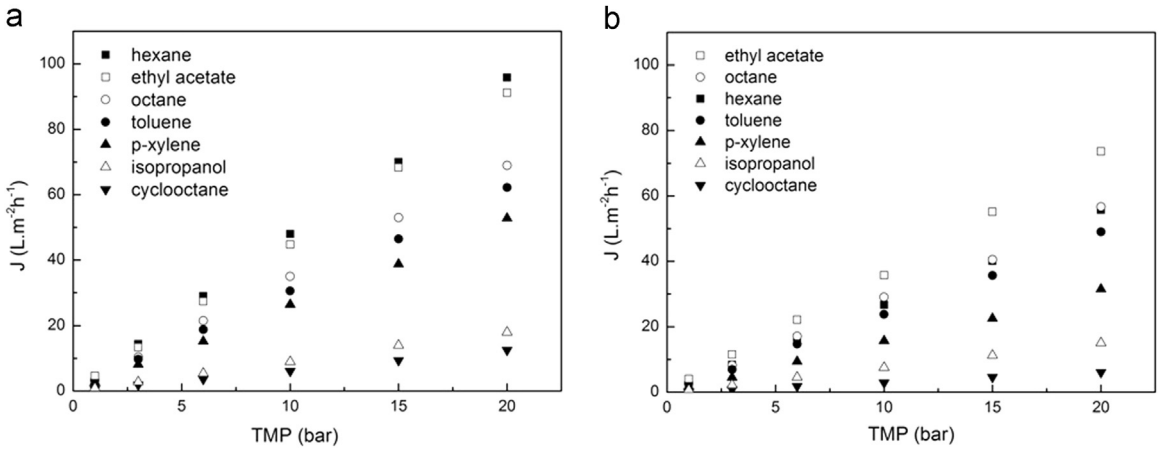

Fig. 2. Pure solvent flux versus TMP for (a) M2 and (b) M3 membranes at 20 °C.

membrane samples for each type of membrane and two measurements for each sample. Standard deviations observed for the fluxes were within 4% error.

As can be seen in Fig. 2, a linear relationship of flux versus TMP was observed for both types of membranes for all solvents, suggesting no effect of compaction. This behavior is in contrast with what is mostly found for pure PDMS polymeric membranes where a non-linear behavior in flux versus TMP is observed due to compaction [16,27]. The linear relationship between the flux and TMP, as observed in our work, also indicates the absence of any shear rate flow-induced behavior as described by Castro et al. [11], who studied the permeability for PVP-grafted porous silica membranes with a native pore diameter of 410 nm. In Castro's work, a more than linear increase of flux (J) as function of TMP was observed, suggesting deformation of the grafted polymeric chains as a result of the shear rate, which increases the effective membrane pore diameter with increasing operational pressure. This difference between the results as described in [11] and those given in Fig. 2 can be explained by the smaller pore size of the ceramic porous support (5 nm) used in this work which might provide higher confinement towards the shear rate effect than for macroporous ceramic supports (410 nm).

If solvent transport in these membranes is according to the viscous-flow or pore-flow model (Hagen– Poiseuille law), an identical slope (k) must be found for all solvents, when flux is plotted versus TMP/μ (μ: solvent viscosity). In that case the membrane permeability constant (k) in Eq. (2) represents the membrane pore geometry, meaning a single value of k should be identified for all solvents since it is assumed that the membrane pore geometry is identical, regardless of the type of permeating solvent used. To validate whether the solvent permeation through the grafted membranes is following the viscous-flow mechanism, fluxes are plotted as function of TMP/μ in Fig. 3.

From the different slopes in Fig. 3, whose values are summarized in Table 3, it can be deduced that for both M2 and M3 permeability is not (or not only) dependent on solvent viscosity.

The pore-flow model does not take into account the interaction between the membrane and the permeating solvent. It is assumed that the membrane pore geometry is constant regardless the type of the permeating solvent. An adapted pore-flow model is now discussed, assuming that permeation is following the viscous flow mechanism, while the membrane pore geometry is varying in the presence of different types of solvent. It is known that PDMS can swell to a large extent in the presence of nonpolar solvents [14,28]. The degree of swelling depends on the affinity between the PDMS and the solvent. Larger swelling means that more solvent molecules are sorbed by PDMS. Swelling can have an influence on the pore geometry of a grafted membrane, because sorption of the solvent molecules by the grafted moiety can decrease the effective membrane permeation volume (porosity and pore size), i.e. the empty space in the central axis of the pores left by the swollen grafted PDMS. It should be noted that molecules, that are responsible for swelling of PDMS, are only loosely interacting with the PDMS chains and should surely not be considered as completely immobile.

This hypothesis can be translated into a modified Hagen–

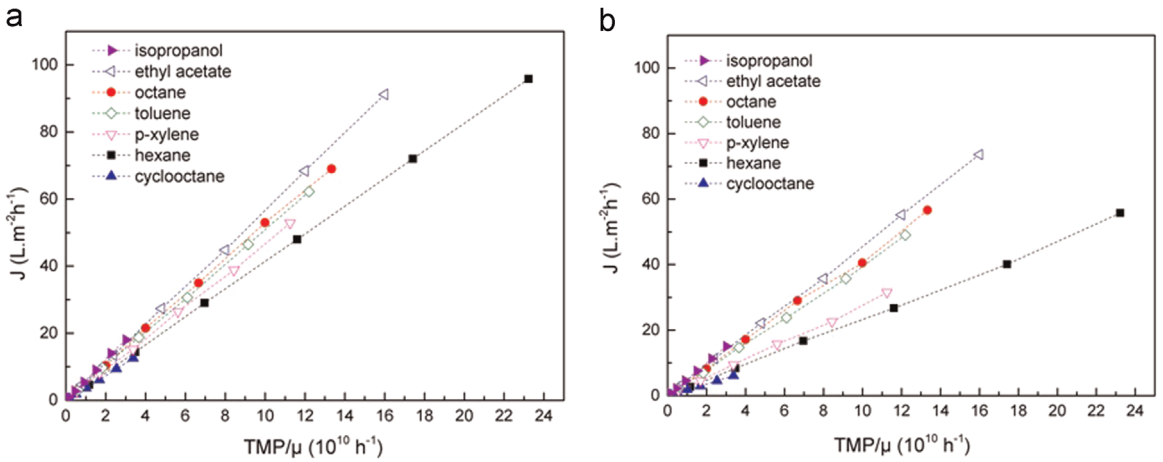

Fig. 3. Fluxes versus the TMP/μ for (a) M2 and (b) M3 membranes at 20 °C.

Table 3
Slopes (k_i) of J versus TMP/μ curves, as given in Fig. 3 for each solvent.

Solvent types	k_i M2	k_i M3
Isopropanol	0.60 ± 0.02	0.50 ± 0.02
Ethyl acetate	0.57 ± 0.02	0.46 ± 0.02
Octane	0.52 ± 0.02	0.43 ± 0.02
Toluene	0.51 ± 0.02	0.40 ± 0.02
p-Xylene	0.47 ± 0.02	0.28 ± 0.01
Hexane	0.41 ± 0.02	0.24 ± 0.01
Cyclooctane	0.37 ± 0.01	0.18 ± 0.01

Poiseuille law. Assuming that the slope in the curve of J versus TMP/μ is different for every solvent due to a change in membrane porosity and pore size when using different solvents, a slope k_i for each solvent i can be determined and by using Eq. (3) we obtain

$$k_i = \frac{\varepsilon_i {r_{p,i}}^2}{8\tau l} \tag{7}$$

where ε_i and $r_{p,i}$ are the actual membrane porosity and pore size in the presence of the permeating solvent i. It is assumed that the membrane porosity and pore size do not have the same value for all solvents, while the other parameters (tortuosity and thickness) do not change significantly with changing solvent.

The permeability constant for each solvent (k_i) can be normalized towards the permeability constant of a reference solvent (k_{ref}). In combination with Eq. (7) this normalized permeability constant (k_i') is expressed as

$$k_i` = \frac{k_i}{k_{ref}} = \frac{\frac{\varepsilon_i {r_{p,i}}^2}{8\tau l}}{\left(\frac{\varepsilon_i {r_{p,i}}^2}{8\tau l}\right)_{ref}} = \frac{V_e}{(V_e)_{ref}} \tag{8}$$

Here an effective permeable volume of the membrane (V_e) is defined (τ and l are identical for all solvents). V_e can be described as the difference between the membrane permeable volume per unit mass of the grafted moiety when there is no solvent present (V_o in cm^3/g) and the volume of sorbed solvent per unit of mass of the grafted moiety (V_s in cm^3/g)

$$V_e = V_o - V_s \tag{9}$$

Combination of Eqs. (8) and (9) gives

$$k_i` = \frac{k_i}{k_{ref}} = \frac{V_e}{(V_e)_{ref}} = \frac{V_o - V_{s,i}}{V_o - V_{s,ref}} \tag{10}$$

The value of V_o is specific for each type of grafted membrane (M2, M3) and depends on the pore volume of the ceramic substrate and the mass of the grafted moiety. The values of $V_{s,i}$ in cm^3/g depends on the type of solvent (the affinity of the solvent with the grafted moiety). $V_{s,ref}$ is the volume of the sorbed solvent per unit mass of the grafted moiety for a reference solvent (cm^3/g).

From here, with a simple mathematical derivation Eq. (10) becomes

$$k_i` = \frac{k_i}{k_{ref}} = \frac{V_o - V_{s,i}}{V_o - V_{s,ref}} = \frac{V_o}{V_o - V_{s,ref}} - \frac{V_{s,i}}{V_o - V_{s,ref}} \tag{11}$$

if

$$V_{s,i}` = \frac{V_{s,i}}{V_{s,ref}} \tag{12}$$

with $V_{s,i}'$ the ratio of the sorption tendency in one solvent relative to that of the reference solvent, or so called the normalized sorption value, then Eq. (11) becomes

$$k_i` = \frac{k_i}{k_{ref}} = \frac{V_o}{V_o - V_{s,ref}} - \frac{V_{s,ref}}{V_o - V_{s,ref}} V_{s,i}` = A - B\, V_{s,i}` \tag{13}$$

with

$$A = \frac{V_o}{V_o - V_{s,ref}} \tag{14}$$

and

$$B = \frac{V_{s,ref}}{V_o - V_{s,ref}} \tag{15}$$

where A is the intercept and B the slope of a plot of $k_i`$ versus $V_{s,i}'$.

Incorporating Eq. (13) in Eq. (2) results in:

$$J_i = k_i \frac{\Delta P}{\mu} = k_{ref}(A - B\, V_{s,i}`)\frac{\Delta P}{\mu} \tag{16}$$

with k_i is the slope of J_i versus TMP/μ for each solvent as a function of $V_{s,i}'$. In this work values of $V_{s,i}$ are obtained through sorption measurements of a PDMS sample in different types of solvent. Crosslinked PDMS samples with a low amount of crosslinker (9% w/w) is chosen as the sample. Table 4 gives the measured sorption values and the sorption values normalized against the sorption of isopropanol, which is chosen as a solvent of reference in this work. In fact, any solvent can be freely chosen as a reference solvent for the calculation of the normalized sorption value.

Possible relations between sorption values and solvent polarity (like dipole moment and dielectric constant) as well as solvent vapor pressure are summarized in Table 4. In general a lower sorption value is observed for polar solvents like isopropanol (dielectric constant of 19.92) or ethyl acetate (dielectric constant of 6.02) if compared to sorption values of nonpolar solvents having dielectric constants between 1.5 and 2.5. A lower sorption value was also found for polar solvents with dipole moments of more than 1.5, while higher sorption values were found for nonpolar solvents with dipole moments less than 0.5. No trend was observed between the sorption value and the vapor pressure of the solvents.

In order to use Eq. (16), the A and B values needs to be

Table 4
Sorption value of a pure PDMS sample with a 9 w/w% of crosslinker at 20 °C and the normalized sorption values against the sorption of isopropanol which is chosen as a solvent of reference.

Solvent	Sorption value $V_{s,i}$ (cm^3/g)	Normalized sorption value $V_{s,i}' = \frac{V_{s,i}}{V_{s,\,isopropanol}}$ (-)	Dipole moment (D)	Dielectric constant (ε)	Vapor pressure (mmHg at 20 °C)
Isopropanol	0.47	1.00	1.66	19.92	78.2
Ethyl acetate	0.48	1.02	1.88	6.02	109.1
Toluene	0.53	1.12	0.34	2.38	26.3
Octane	0.54	1.15	0.00	1.95	13.9
p-Xylene	0.63	1.34	0.07	2.27	7.6
Hexane	0.66	1.40	0.08	1.89	129.1
Cyclooctane	0.70	1.48	0.00	2.12	4.4

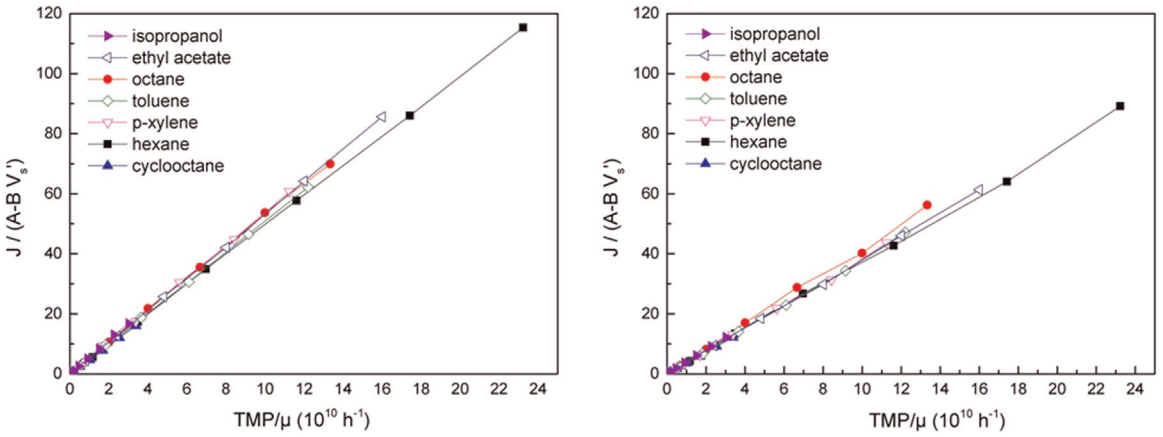

Fig. 4. Plot of J corrected with $(A - BV_{s,i}')$ against TMP/μ at 20°C.

determined. The A and B are obtained by a the k_i` is versus $V_{s,i}'$ plot. according to Eq. (13). In this way for membrane M2 $A$ and $B$ values of respectively $1.68 \pm 0.07$ and $0.68 \pm 0.09$ were calculated while for membrane M3 $A$ and $B$ values were respectively $2.27 \pm 0.09$ and $1.27 \pm 0.07$. Details on $k_i$` versus $V_{s,i}'$ are given in the appendix to this paper. If k_i is corrected with $(A - BV_{s,i}')$, then, according to Eq. (16), the slopes in the curve of flux versus TMP/μ will unite into a single slope, which is equal to k_{ref}. The plot of the flux/$(A - BV_{s,i}')$ versus TMP/μ for M2 and M3 membranes are given in Fig. 4.

From Fig. 4, it can be seen that almost a single slope is formed when J corrected with $(A - BV_{s,i}')$ is plotted against TMP/μ in accordance to Eq. (13). The applicability of this equation for describing the solvent permeation of these porous grafted ceramic membranes indicates that the solvent permeability of grafted membranes is governed by the solvent sorption tendency of the grafted moiety aside from the solvent viscosity. The slopes of $J/(A - BV_{s,i}')$ versus TMP/μ as given in Fig. 4 for each solvent including the error values are presented in Table 5 for M2 and M3 approaching the k_{ref}.

4.3. Flux as function of temperature

In order to check whether similar major parameters affect membrane permeability at elevated temperatures, permeability tests were done in the temperature range of 20–70 °C and given in Fig. 5.

It can be seen from Fig. 5 that the flux increases with increasing temperature. The increased movements of individual molecules at higher temperature reduce the intermolecular forces resulting in a

Table 5
Slopes of $J/(A - BV_{s,i}')$ versus TMP/μ as given in Fig. 4 for each solvent indicating the k_{ref} values.

Solvent types	Slopes M2	Slopes M3
Isopropanol	0.60 ± 0.02	0.50 ± 0.02
Ethyl acetate	0.58 ± 0.02	0.47 ± 0.03
Octane	0.58 ± 0.02	0.53 ± 0.02
Toluene	0.56 ± 0.03	0.47 ± 0.04
p-Xylene	0.61 ± 0.03	0.49 ± 0.02
Hexane	0.56 ± 0.03	0.49 ± 0.03
Cyclooctane	0.55 ± 0.03	0.46 ± 0.02

Table 6
Solvent viscosity at elevated temperatures [29]

T (°C)	Viscosity μ (mPa s)		
	Octane	Toluene	Isopropanol
20	0.54	0.59	2.39
30	0.48	0.52	1.88
40	0.43	0.48	1.45
50	0.39	0.45	1.20
60	0.35	0.43	0.89
70	0.33	0.42	0.82

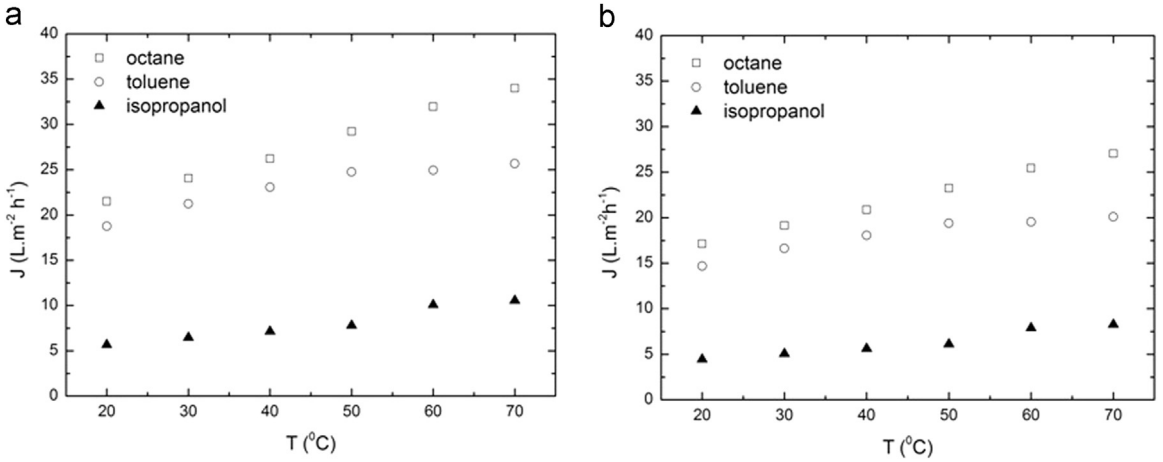

Fig. 5. Flux versus temperature at a constant TMP of 6 bar for (a) M2 and (b) M3 membranes.

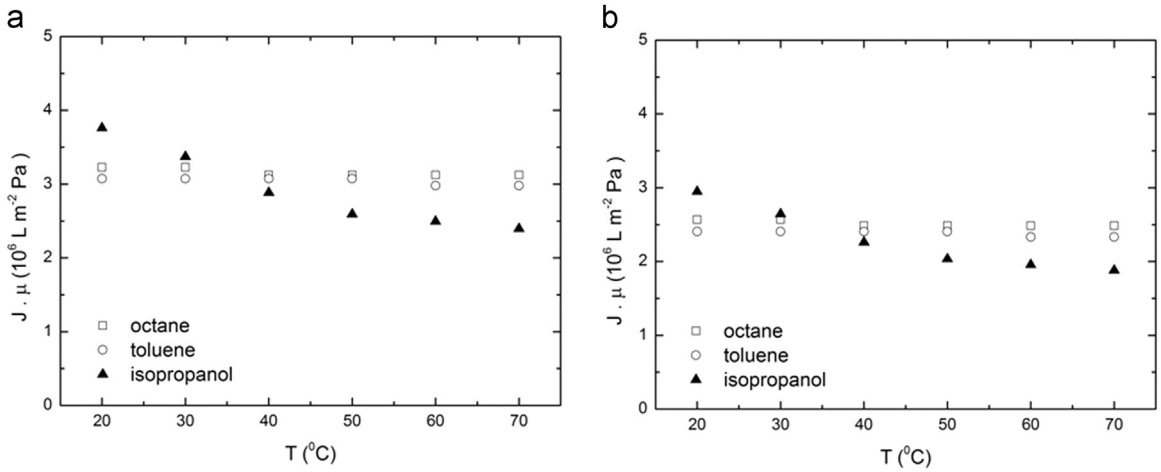

Fig. 6. Solvent fluxes corrected for the solvent viscosity versus T for (a) M2 and (b) M3 membranes.

Table 7
Sorption values of PDMS samples as function of temperature.

T (°C)	Sorption values $V_{s,T}$(cm^3/g)			Normalized sorption values $V_{S,T'} = \frac{V_{S,T}}{V_{S,20\,°C,isopropanol}}$(-)		
	Octane	Toluene	Isopropanol	Octane	Toluene	Isopropanol
20	0.54	0.53	0.47	1.15	1.13	1.00
30	0.54	0.53	0.51	1.15	1.13	1.09
40	0.55	0.53	0.56	1.17	1.13	1.19
50	0.55	0.53	0.59	1.17	1.13	1.26
60	0.55	0.54	0.60	1.17	1.15	1.28
70	0.55	0.54	0.61	1.17	1.15	1.30

decrease of solvent viscosity. Besides, there is also an enhanced polymer chain mobility at elevated temperatures. The solvent viscosities as function of temperature are given in Table 6.

The viscosity corrected flux, according to Darcy's law, are plotted in Fig. 6 as a function of permeation temperature.

It can be seen from Fig. 6 that the permeability of isopropanol decreases for both membranes with increasing temperature after being corrected for the solvent viscosity at the pertinent temperatures. For octane and toluene on the other hand, the viscosity corrected flux was found to be constant with the increase in temperature.

The differences in permeability behavior as function of temperature between octane and toluene on one side and isopropanol on the other side might indicate a difference in sorption behavior of PDMS in the different solvents for the studied temperature range. Table 7 shows the sorption values ($V_{S,T}$) of PDMS at different temperatures for the respective solvents.

A significant dependency of the sorption value with temperature is observed for PDMS-isopropanol systems. For PDMS-octane and PDMS-toluene systems it was found that sorption values only slightly depend on temperature. The increasing sorption of isopropanol in the grafted moiety at increasing temperature might be the reason for the decrease in isopropanol permeability with increasing temperature, as shown in Fig. 6(a) and (b). In order to check whether solvent sorption also affects the solvent transport through grafted membranes as function of temperature, the viscosity corrected flux is further on corrected for the sorption of solvent at the pertinent temperature according to (see also Eq. (16))

$$\frac{J.\mu}{(A - B.\ V_{S,T`})} = k_{ref}.\ \Delta P \tag{17}$$

If similar parameters affecting the membrane permeability as function temperatures, $\frac{J.\mu}{(A-B.\ V_{S,T`})}$ should be constant against the permeation temperature.

The fluxes corrected with the $\frac{1}{A-B.V_{S,T`}}$ for each membrane types plotted against the permeation temperature are given in Fig. 7.

As can be seen from Fig. 7 Eq. (17) can be applied for describing

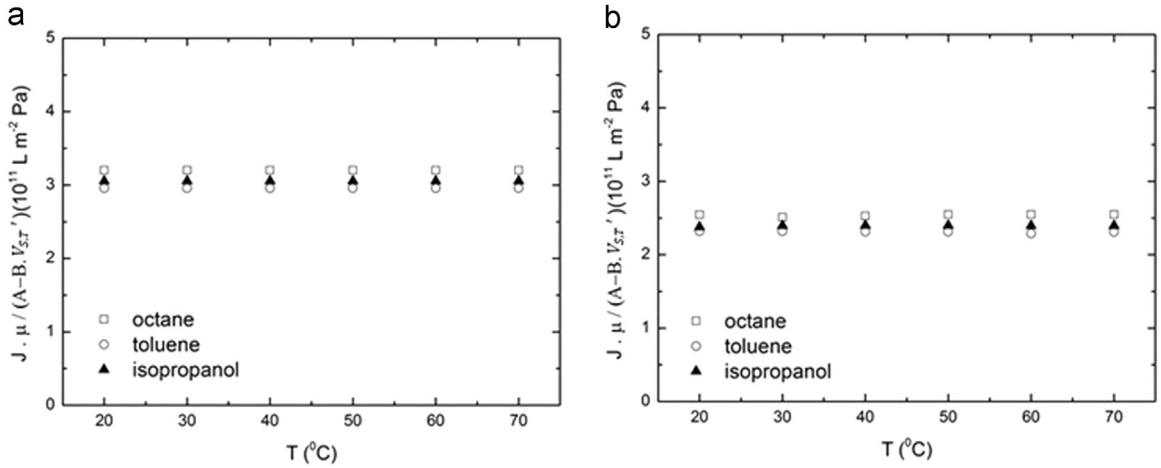

Fig. 7. The fluxes corrected with $\frac{1}{A-B.V_{S,T`}}$ plotted against the permeation temperature using A and B values calculated previously for (a) M2 and (b) M3 membranes.

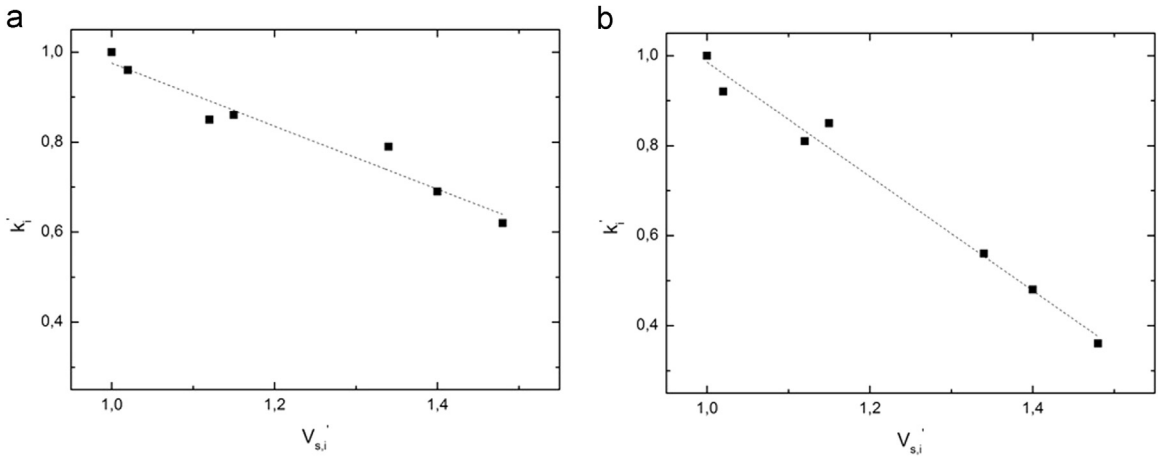

Fig. A1. Plot of k_i' versus $V_{s,i}'$ for a) M2 and b) M3 membranes. .

the membrane permeability behavior. From all these results it can be concluded that the permeability of PDMS-grafted γ-alumina ceramic membranes, as studied in this work, is dominated by the solvent viscosity and the solvent sorption of the grafted moiety in a solvent when used in a temperature range of 20–70 °C.

5. Conclusions

Prepared PDMS-grafted alumina membranes are stable for permeation of different types of solvents for at least 10 days. No compaction or shear flow-induced behavior was observed during solvent transport through the grafted membranes at trans-membrane pressures up to 20 bars. The solvent permeation of these ceramic membranes was found to be mainly governed by Darcy's and Hagen–Poiseuille law, but with taking into account swelling of the grafted moiety. An empirical model, derived from the Hagen–Poiseuille model, using the sorption tendency of the grafted material in different solvents, can be used to describe the membrane permeability behavior.

Acknowledgment

The authors acknowledge financial support from the European Union—The Education, Audiovisual and Culture Executive Agency (EACEA) under the Program Erasmus Mundus Doctorate in Membrane Engineering—EUDIME (FPA 2011-2014) and an I.A.P. Grant sponsored by the Belgian Federal Government.

Appendix A

See Fig. A1

Appendix A. Supplementary material

Supplementary data associated with this article can be found in the online version at doi:10.1016/j.memsci.2015.08.004.

References

[1] P. Vandezande, L.E.M. Gevers, I.F.J. Vankelecom, Solvent resistant nanofiltration: separating on a molecular level, Chem. Soc. Rev. 37 (2008) 365–405.
[2] C. Leger, H.L. De Lira, R. Paterson, Preparation and properties of surface modified ceramic membranes. Part II. Gas and liquid permeabilities of 5 nm alumina membranes modified by a monolayer of bound polydimethylsiloxane (PDMS) silicone oil, J. Membr. Sci. 120 (1996) 135–146.
[3] R.S. Faibish, Y. Cohen, Fouling-resistant ceramic-supported polymer membranes for ultrafiltration of oil-in-water microemulsions, J. Membr. Sci. 185 (2001) 129–143.
[4] W. Yoshida, Y. Cohen, Ceramic-supported polymer membranes for pervaporation of binary organic/organic mixtures, J. Membr. Sci. 213 (2003) 145–157.
[5] W. Yoshida, Y. Cohen, Removal of methyl tert-butyl ether from water by pervaporation using ceramic-supported polymer membranes, J. Membr. Sci. 229 (2004) 27–32.
[6] K.C. Popat, G. Mor, C.A. Grimes, T.A. Desai, Surface modification of nanoporous alumina surfaces with poly(ethylene glycol), Langmuir 20 (2004) 8035–8041.
[7] L. Sang Won, S. Hao, T.H. Richard, P. Vania, U.L. Gil, Transport and functional behaviour of poly(ethylene glycol)-modified nanoporous alumina membranes, Nanotechnology 16 (2005) 1335.
[8] A.F.M. Pinheiro, D. Hoogendoorn, A. Nijmeijer, L. Winnubst, Development of a PDMS-grafted alumina membrane and its evaluation as solvent resistant nanofiltration membrane, J. Membr. Sci. 463 (2014) 24–32.
[9] C.R. Tanardi, A.F.M. Pinheiro, A. Nijmeijer, L. Winnubst, PDMS grafting of mesoporous γ-alumina membranes for nanofiltration of organic solvents, J. Membr. Sci. 469 (2014) 471–477.
[10] R.P. Castro, Y. Cohen, H.G. Monbouquette, The permeability behavior of polyvinylpyrrolidone-modified porous silica membranes, J. Membr. Sci. 84 (1993) 151–160.
[11] R.P. Castro, H.G. Monbouquette, Y. Cohen, Shear-induced permeability changes in a polymer grafted silica membrane, J. Membr. Sci. 179 (2000) 207–220.
[12] S. Aerts, A. Vanhulsel, A. Buekenhoudt, H. Weyten, S. Kuypers, H. Chen, M. Bryjak, L.E.M. Gevers, I.F.J. Vankelecom, P.A. Jacobs, Plasma-treated PDMS-membranes in solvent resistant nanofiltration: characterization and study of transport mechanism, J. Membr. Sci. 275 (2006) 212–219.
[13] L.E.M. Gevers, I.F.J. Vankelecom, P.A. Jacobs, Solvent-resistant nanofiltration with filled polydimethylsiloxane (PDMS) membranes, J. Membr. Sci. 278 (2006) 199–204.
[14] L.E.M. Gevers, I.F.J. Vankelecom, P.A. Jacobs, Zeolite filled polydimethylsiloxane (PDMS) as an improved membrane for solvent-resistant nanofiltration (SRNF), Chem. Commun. (2005) 2500–2502.
[15] M. Mulder, Basic Principles of Membrane Technology, 2nd ed., Kluwer Academic Publisher, Netherlands, 1996.
[16] I.F.J. Vankelecom, K. De Smet, L.E.M. Gevers, A. Livingston, D. Nair, S. Aerts, S. Kuypers, P.A. Jacobs, Physico-chemical interpretation of the SRNF transport mechanism for solvents through dense silicone membranes, J. Membr. Sci. 231 (2004) 99–108.
[17] J.G. Wijmans, R.W. Baker, The solution-diffusion model: a review, J. Membr. Sci. 107 (1995) 1–21.
[18] J. Wang, D.S. Dlamini, A.K. Mishra, M.T.M. Pendergast, M.C.Y. Wong, B. B. Mamba, V. Freger, A.R.D. Verliefde, E.M.V. Hoek, A critical review of transport through osmotic membranes, J. Membr. Sci. 454 (2014) 516–537.
[19] G. Jonsson, Overview of theories for water and solute transport in9 UF/RO membranes, Desalination 35 (1980) 21–38.
[20] J.P. Robinson, E.S. Tarleton, C.R. Millington, A. Nijmeijer, Solvent flux through dense polymeric nanofiltration membranes, J. Membr. Sci. 230 (2004) 29–37.
[21] S. Zeidler, U. Kätzel, P. Kreis, Systematic investigation on the influence of solutes on the separation behavior of a PDMS membrane in organic solvent nanofiltration, J. Membr. Sci. 429 (2013) 295–303.
[22] S. Postel, G. Spalding, M. Chirnside, M. Wessling, On negative retentions in organic solvent nanofiltration, J. Membr. Sci. 447 (2013) 57–65.
[23] A. Nijmeijer, B.J. Bladergroen, H. Verweij, C.V.I. Low-temperature, modification of γ-alumina membranes, Micropor. Mesopor. Mater. 25 (1998) 179–184.
[24] F.P. Cuperus, D. Bargeman, C.A. Smolders, Permporometry: the determination

of the size distribution of active pores in UF membranes, J. Membr. Sci. 71 (1992) 57–67.
[25] P. Vandezande, L.E.M. Gevers, J.S. Paul, I.F.J. Vankelecom, P.A. Jacobs, High throughput screening for rapid development of membranes and membrane processes, J. Membr. Sci. 250 (2005) 305–310.
[26] X. Li, F. Monsuur, B. Denoulet, A. Dobrak, P. Vandezande, I.F.J. Vankelecom, Evaporative light scattering detector: toward a general molecular weight cutoff characterization of nanofiltration membranes, Anal. Chem. 81 (2009) 1801–1809.
[27] D.R. Paul, J.D. Paciotti, O.M. Ebra-Lima, Hydraulic permeation of liquids through swollen polymeric networks. II. Liquid mixtures, J. Appl. Polym. Sci. 19 (1975) 1837–1845.
[28] J.N. Lee, C. Park, G.M. Whitesides, Solvent compatibility of poly(dimethylsiloxane)-based microfluidic devices, Anal. Chem. 75 (2003) 6544–6554.
[29] R.H. Perry, D.W. Green, J.O. Maloney, M.M. Abbott, C.M. Ambler, R.C. Amero, Perry's Chemical Engineers' Handbook, McGraw-Hill, New York, 1997.
[30] D. Lide, CRC Handbook of Chemistry And Physics: A Ready-reference Book Of Chemical And Physical Data, in: D.R. Lide, F.L. Boca Raton, C.R.C. Press (Eds.), 2002.
[31] T.E. Daubert, R.P. Danner, Physical and Thermodynamic Properties of Pure Chemicals: Design institute for Physical Property Data, American Institute of Chemical Engineers, Hemisphere Publishing Corporation, New York (NY), 1989.
[32] J.A. Dean, Lange's Handbook of Chemistry, McGraw-Hill, New York, 1999.
[33] W.J. Cannella, Xylenes and Ethylbenzene, Kirk-Othmer Encyclopedia of Chemical Technology, John Wiley and Sons, Inc., 2000.
[34] J.E. Logsdon, R.A. Loke, Isopropyl Alcohol, Kirk-Othmer Encyclopedia of Chemical Technology, John Wiley and Sons, Inc., 2000.
[35] A.F.M. Pinheiro, Development and characterization of polymer-grafted ceramic membranes for solvent nanofiltration (PhD thesis),, University of Twente, Enschede, 2013.